PCCP

Hydrogen-induced high-temperature segregation in palladium silver membranes

Journal:	*Physical Chemistry Chemical Physics*
Manuscript ID:	CP-ART-07-2014-003245.R1
Article Type:	Paper
Date Submitted by the Author:	03-Oct-2014

Complete List of Authors:	Zeng, Gaofeng; Shanghai Advanced Research Institute, Jia, Haiyuan; Dalian Institute of Chemical Physics, CAS, Dalian National Laboratory for Clean Energy Goldbach, Andreas; Dalian Institute of Chemical Physics, CAS, Dalian National Laboratory for Clean Energy Zhao, Lingfang; Dalian Institute of Chemical Physics, CAS, Dalian National Laboratory for Clean Energy Miao, Shu; Dalian Institute of Chemical Physics, Shi, Lei; Shanghai Institute of Microsystem and Information Technology, State Key Laboratory of Functional Materials for Informatics Sun, Chenlin; Dalian National Laboratory for Clean Energy, Dalian Institute of Chemical Physics, Chinese Academy of Sciences Xu, Hengyong; Dalian Institute of Chemical Physics, Laboratory of Applied Catalysis

Cite this: DOI: 10.1039/c0xx00000x

www.rsc.org/xxxxxx

ARTICLE TYPE

Hydrogen-induced high-temperature segregation in palladium silver membranes

Gaofeng Zeng,[a,b,‡] Haiyuan Jia,[a,‡] Andreas Goldbach,[a,*] Lingfang Zhao,[a] Shu Miao,[a] Lei Shi,[a,c] Chenglin Sun,[a] and Hengyong Xu[a,*]

Received (in XXX, XXX) XthXXXXXXXXX 20XX, Accepted Xth XXXXXXXXX 20XX
DOI: 10.1039/b000000x

Higher operation temperatures benefit H_2 permeability and selectivity of metal membranes and they are interesting for e.g. water gas shift and steam reforming in membrane reactors. Hence the behaviour of PdAg/ceramic composite membranes has been investigated between 823 K and 923 K. The H_2 flux of membranes with less than 10 µm thick alloy layers decreased continuously with time during operation under H_2 at 873 K and above. This was accompanied by a steady increase of the activation energy for H_2 permeation and the growth of Ag-depleted crystallites on the membrane surface. All phenomena could be reversed through annealing under N_2 at 923 K. The textural and permeability changes are consistent with a segregation mechanism starting with metal sublimation from hydrogenated PdAg layers and subsequent metal resublimation. This implies an enhancement of the yet unknown metal activities in PdAg hydride phases over metallic PdAg alloys. Ramifications for application of thin-layered, supported PdAg membranes for H_2 separation above 823 K are discussed.

1. Introduction

Pd-based membranes are promising tools for production of high-purity hydrogen when economics prohibit the application of industrially established large-scale purification technologies such as pressure swing adsorption.[1] They can be also integrated into reactors for a wide range of H_2-involving processes to drive conversions beyond thermodynamic limits.[2] PdAg alloys are most widely investigated for these purposes because they exhibit higher hydrogen permeabilities than pure Pd with optimum around 23% Ag[3,4] and allow cost reduction due to substitution of Pd with much less expensive Ag. In addition, the α/β hydride miscibility gap is lowered below room temperature at higher Ag concentrations[5] reducing the propensity for embrittlement. In recent years much attention has been paid to ultrathin PdAg layers (supported on porous ceramic or metal substrates for mechanical stability) in order to improve membrane permeability and economics further.[6,7] Questions remain about the performance of such membranes at elevated temperatures, i.e. above 723 K.[8] Higher temperatures benefit H_2 permeability and selectivity of metal membranes in general and they facilitate alloy formation during membrane preparation if Pd and Ag are separately deposited.[9-11] They are also attractive for water gas shift reaction[12] and steam reforming of natural gas[13] in membrane reactors.

However, some studies have indicated that the H_2 permeability of supported PdAg membranes declines at higher temperatures due to reduction of ceramic substrates (α-Al_2O_3) and subsequent formation of less permeable PdAl alloys,[14] intermetallic diffusion if metal supports without diffusion barriers are used,[15] or surface enrichment with Ag.[16] In general Ag accumulates on PdAg surfaces because of its lower surface tension in comparison to Pd[17] but experimental[18,19] and theoretical studies[20-22] suggest that Pd segregates to the surface of PdAg alloys under H_2 exposure. Practically, Ag enrichment has been observed on surfaces of supported PdAg membranes operated in H_2 for long times[23-25] though this Ag excess decreased with increasing temperature.[24,25]

Since the high-temperature picture remains unclear we revisited the behaviour of thin-layered PdAg membranes supported on ceramic microfiltration membranes under those conditions. In particular, we investigated how permeation and surface characteristics are affected under H_2 separation conditions focusing on hydrogen-induced changes and their reversibility. Aforementioned high-temperature mechanisms[14-16] can be ruled out as cause of observed textural changes in the present case on basis of our surface analyses. Instead we propose that hydrogen incorporation facilitates metal sublimation from PdAg alloys which has general implications for the operability of thin-layered PdAg membranes at elevated temperatures.

2. Experimental section

2.1 Membrane Preparation

Table 1 provides an overview of the membranes used in this study. Preparation of PdAg layers via sequential electroless plating of Pd and Ag on the outside of ceramic membranes has been previously described in detail including cleaning of support, support activation and Pd deposition using commercial solutions (Okuno Chemical Industries) and Ag deposition from home-made plating baths.[11,26] Here, porous α-Al_2O_3 tubes (Nanjing

University of Technology) were used as support with inner and outer diameters of 8 and 12 mm, a 15 μm thick γ-Al_2O_3 intermediate layer and a 15 μm thick ZrO_2 top layer on the outside.[26] Two sealing methods were used. Either, ca. 50 mm long PdAg layers were deposited on otherwise glazed supports as reported elsewhere,[26] or ca. 100 mm long membranes were connected via graphite (graph) seals with an end-cap and extension tube made of stainless steel after Pd and Ag deposition. As-prepared Pd-Ag bi-layers were heated in N_2 to 573 K before switching to H_2. Membranes were heated to 673 K for initial alloying (4 h, N_2) of the metal layers prior to application of graphite seals.

Table 1. Membrane characteristics with overall Ag concentrations derived from XRD, EDX and XPS analyses after operation under H_2.

Membrane (seal type)	Area	PdAg thickness		Ag concentration			$\alpha_{H2/N2}$[a]
		ΔW	SEM	XRD	EDX	XPS	
	cm^2	μm	μm	at.%	at.%	at.%	
M1 (glaze)	18.8	2.6	1.9-3.0	27.6	22.7	41.2	5680
M2 (glaze)	18.8	2.9	3.1-3.6	21.6	19.6	33.1	1674[b]
M3 (graph)	18.1	4.7	2.3-2.6	13.0	13.3	23.8	198
M4 (graph)	16.8	6.4	4.2-5.3	24.6	20.2	37.0	469
M5 (graph)	17.7	3.2	/	/	/	/	375

[a]at 823 K and ΔP = 100 kPa; [b]at 873 K and ΔP = 100 kPa.

2.2 Membrane annealing and testing

Annealing and permeation experiments were carried out in previously described shell-tube permeation setups.[27] Membranes were mounted using graphite gaskets and Teflon O-rings at the cold ends of the glazed support or extension tube, respectively. Hydrogen or nitrogen was fed to the membrane shell side while the tube interior was kept at atmospheric pressure and no sweep gas was used. The feed side was also kept at atmospheric pressure during annealing while supplying H_2 or N_2 at constant rates between 140 ml min^{-1} and 190 ml min^{-1}. Single gas H_2 and N_2 fluxes J_{H2} and J_{N2}, respectively, were measured feeding 1800-3500 ml min^{-1} H_2 or 300-500 ml min^{-1} N_2 at pressure differences up to ΔP = 100 kPa. From these ideal H_2/N_2 selectivity $\alpha_{H2/N2} = J_{H2}/J_{N2}$ was calculated. During annealing in H_2 or N_2, permeation measurements with the alternate feed gas were carried out swiftly to minimize exposure of the membrane to the alternate atmosphere. Activation energies for H_2 permeation E_{act} were determined from measurements at three temperatures between 623 K and annealing temperature. The temperature was changed at a rate of 2 K min^{-1} and then held at least 10 min before H_2 flux measurements were started. Reported permeation rates were measured at ΔP = 100 kPa unless otherwise noted. The purity of H_2 and N_2 was 99.999% except for experiments with membranes M3-M5 where technical grade H_2 (99%) was used.

2.3 Membrane characterization

The membranes were broken for analysis after conclusion of permeation tests. Alloy crystal structure and composition were determined by X-ray diffraction (XRD, PANalytical X'Pert) using Cu Kα radiation (λ = 0.15406 nm, 40 kV, 40 mA) and a previously reported correlation between lattice constant and alloy stoichiometry.[26] Membrane fragments were further characterized by scanning electron microscopy (SEM, on FEI Quanta 600G and JEOL JSM-7800F instruments) and energy dispersive X-ray spectroscopy (EDX) at an accelerating voltage of 15 or 30 kV. Membrane thickness was also estimated from weight gain (ΔW) after metal deposition. The near-surface compositions of membrane fragments were analysed by X-ray photoelectron spectroscopy (XPS) using Thermo Scientific ESCALAB 250Xi (Al Kα radiation, 1486.6 eV, 15 kV, 10.8 mA) and K-Alpha (Al Kα radiation, 1486.6 eV, 12 kV, 3 mA) X-ray photoelectron spectrometers. Sputter depth profiling was carried on the K-Alpha instrument using Ar^+ ions with 30º beam incidence. The ion gun was operated at 3×10^{-6} Pa, 2 keV and 45 μA cm^{-2} which resulted in sputtering rates of approximately 15 nm min^{-1}. XPS peak positions were calibrated with the help of the C1s peak at 285.0 eV which originated from carbon contaminations contracted during handling of the samples on air. Alloy compositions are given in atom % throughout this paper.

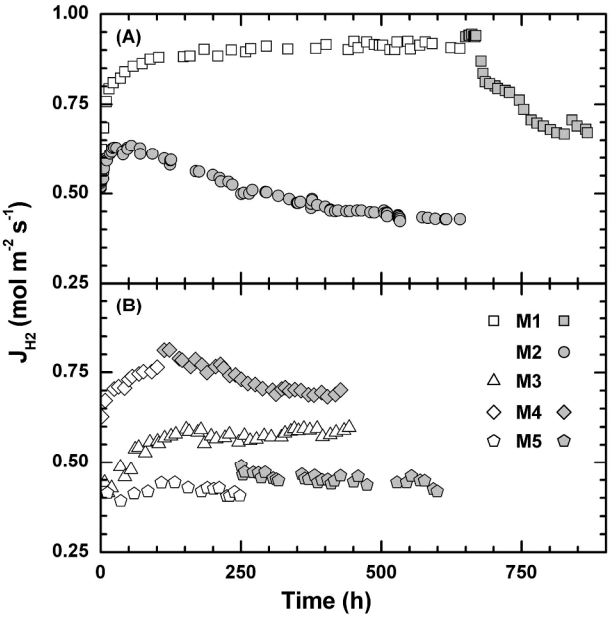

Fig. 1 Hydrogen fluxes (at ΔP_{H2} = 100 kPa) during annealing of (A) glazed and (B) graphite-sealed membranes at 823 K (open symbols) and 873 K (filled symbols). Fluxes of membrane M5 where measured at ΔP_{H2} = 50 kPa and data of membrane M4 have been offset by +0.25 mol m^{-2} s^{-1} for clarity of display.

3. Results

3.1 High-temperature permeation

Fig. 1 shows H_2 fluxes measured during annealing of four PdAg (M1-M4) and one Pd membrane (M5) under H_2 at 823 K and 873 K. Fluxes of the PdAg membranes increased initially due to alloying of the precursor Pd-Ag bi-layers but became stable at 823 K (M1, M3) as soon as a largely homogeneous alloy layer had formed. In contrast, J_{H2} of membrane M2 rapidly reached a maximum during annealing at 873 K and then declined steadily. Hydrogen fluxes also started to decrease soon after raising the temperature of membranes M1 and M4 from 823 K to 873 K, dropping continuously and substantially below the values measured at lower temperature. The pure Pd membrane exhibited stable H_2 fluxes at both temperatures on the other hand, with J_{H2} being somewhat larger at 873 K as expected for a temperature-activated transport process. Thus, deterioration of the

metal/ceramic composite structure can be ruled out as cause of the PdAg membranes' permeability decline at 873 K.

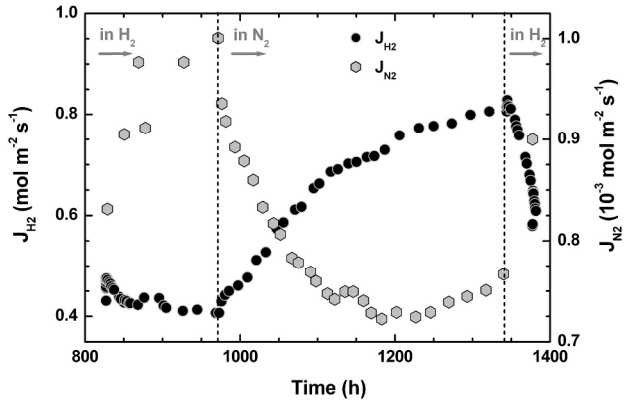

Fig. 2 H_2 and N_2 fluxes at ΔP_{H2} = 100 kPa during annealing of membrane M2 at 923 K in H_2 and N_2.

When the annealing temperature of membrane M2 was raised further to 923 K while still under H_2, J_{H2} increased a little initially but then proceeded to dwindle (Fig. 2). However, J_{H2} started to rebound immediately when H_2 was removed and annealing continued under N_2 instead. The H_2 permeation rate approached a stable level after 380 h operation in N_2 which was twice as high as the one before the atmosphere switch. J_{H2} started to decrease rapidly again when the annealing atmosphere was shifted back to H_2 after 1345 h. These observations clearly demonstrate that hydrogen itself has a retarding effect on H_2 permeability of PdAg membranes at 873 K and above. Curiously, J_{N2} was conversely affected by these atmospheric shifts (Fig. 2). It grew by ca. 20% while the membrane was kept under H_2 at 923 K but began to recede as soon as N_2 was introduced dropping even below its starting value at that temperature before eventually growing again. Thus, H_2/N_2 selectivity increased from ca. 400 to more than 1000 during annealing under N_2. The leak rate growth accelerated again after returning to the H_2 annealing atmosphere.

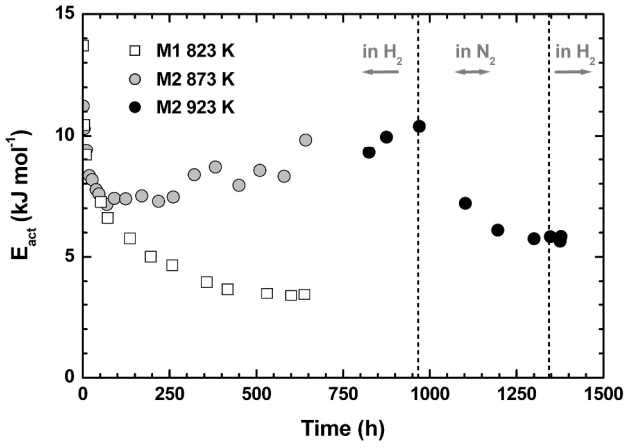

Fig. 3 Activation energies for H_2 permeation during annealing of membranes M1 and M2 in H_2 and N_2, respectively.

The activation energy for H_2 permeation is very sensitive to PdAg alloy composition and homogeneity.[4,11] Fig. 3 shows that E_{act} decreased continuously during annealing of membrane M1 at 823 K becoming steady at 3.4 kJ mol^{-1} after 640 h. This trend is typical during alloying of Pd and Ag and reflects that the overall permeation rate and corresponding energetics are governed by the slowest permeation kinetic step. That is transport through the Ag-rich layer at the membrane surface. The energetic diffusion barrier was highest for the initially pure Ag layer but became lower and lower as its Ag content decreased upon Pd-Ag inter-diffusion until a homogeneous PdAg layer had been formed. The final activation energy of membrane M1 after annealing at 823 K is characteristic for well-alloyed PdAg membranes with ca. 23% Ag.[4] At the beginning E_{act} decreased also rapidly during annealing of membrane M2 at 873 K but it seemed to stabilize around 7.2 kJ mol^{-1} after only 2 days and eventually increased again slowly, reaching 10.4 kJ mol^{-1} after 970 h operation in H_2 (Fig. 3). This trend was reversed when the atmosphere was shifted to N_2 and the activation energy declined once more concomitant with the growing H_2 permeation rate. It dropped to E_{act} = 5.8 kJ mol^{-1} before switching the annealing atmosphere back to H_2. These observations insinuate that compositional homogeneity of the PdAg layer was not reached and even became worse during annealing in H_2 at 873 K and above.

3.2 Microstructural and elemental analyses

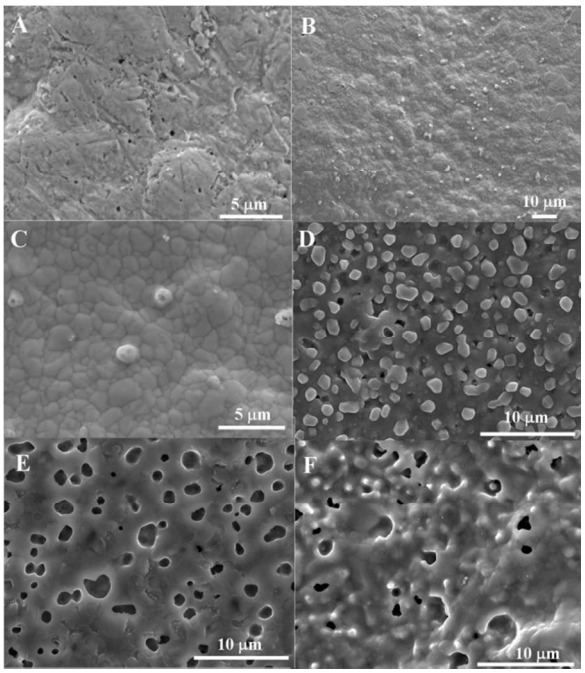

Fig. 4 SEM surface images of PdAg membranes: (A) M3 after annealing in H_2 at 823 K, (B) and (C) M4 after annealing in H_2 at 873 K, (D) M1 after annealing in H_2 at 873 K, (E) M1 after additional annealing in N_2 at 873 K, and (F) M2 after alternating annealing in H_2 and N_2 at 873-973 K.

Fig. 4 displays SEM images of the PdAg membranes at the end of the H_2 annealing treatments shown in Fig. 1 and (for M2) Fig. 2 unless otherwise noted. Membrane M3 had been operated at 823 K only and its surface was coarse and dented with many pinholes after this treatment (Fig. 4A). In contrast, the surface of membrane M4 exhibited a grainy texture and was littered with up to 2 μm wide crystalline particles following annealing under H_2 at 873 K (Fig. 4B and 4C). Similarly, polygonal protrusions dominated the surface of membrane M1 (Fig. 4D) interspersed with some gaping holes after it had been operated twice as long as M4 under H_2, though duration of the final treatment at 873 K

had been comparable for both membranes (240 h vs. 330 h). Those protrusions had disappeared following annealing of another M1 fragment for an additional 150 h in N_2 at 873 K leaving large blind holes behind (Fig. 4E). Finally, the surface morphology of membrane M2 was rugged with rounded protrusions and many large pits after alternate operation in H_2 and N_2 between 873 and 923 K for more than 2 months (Fig. 4F).

These images demonstrate that the surface morphology of PdAg membranes is strongly affected by operating atmosphere and temperature. The surface apparently remained close to the as-prepared state under H_2 at 823 K whereas it completely recrystallized with distinctive grain growth and segregation of crystallites when the temperature was raised by 50 K. Evidently this transformation was driven by hydrogen as the crystallites dissolved into the underlying surface again when kept under N_2. Annealing time of the M1 fragment in N_2 at 873 K was likely too short for the crystallites to deliquesce completely and spread out evenly on the surface so that blind holes formed in crystallite-free zones. On the other hand, some membrane defects may have been covered during this dissolution process accounting for the declining membrane leak flow while annealing under N_2.

Table 1 details alloy stoichiometries determined at the end of the H_2 annealing treatments shown in Fig. 1 and (for M2) Fig. 2. Silver concentrations derived from XRD lattice constants and large area EDX scans such as Fig. 4B are bulk values due to the analysis depths of these methods for PdAg alloys, i.e. ca. 1 µm for EDX and ca. 2 µm for XRD. Yet, EDX values are noticeably lower than XRD ones for membranes annealed at 873-923 K while both values are very close for M3 which was only operated at 823 K. Also, EDX analysis yielded 28.2 at.% Ag for the M1 fragments annealed under N_2 (Fig. 4E) in good agreement with the M1 XRD analysis (27.6 at.%.). These analyses point at Ag depletion towards the membrane surface under H_2 at 873 K and above while operation under N_2 or at lower temperature in H_2 allowed homogenization of the whole alloy layer.

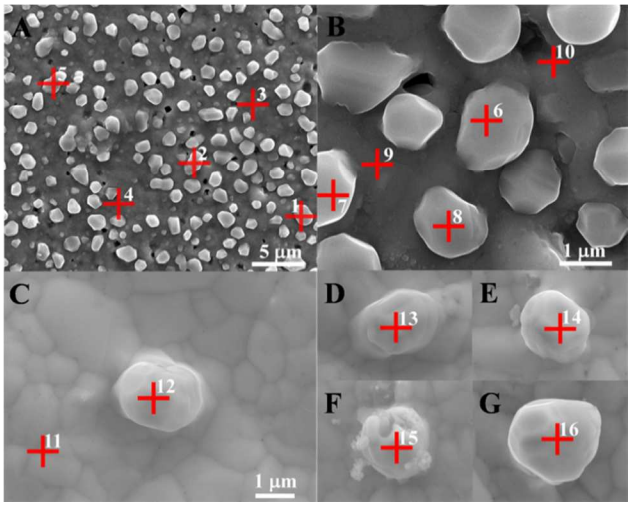

Fig. 5 Segregated crystallites and crystallite-free regions on PdAg membranes M1 (A,B) and M4 (C-G) subjected to EDX spot analyses. The scale bar in image (C) applies also for images (D-G).

The composition of segregated crystallites and crystallite-free regions on membranes M1 and M4 was analysed by EDX in addition. Particles and locations subjected to spot analyses are indicated in Fig. 5 and Ag contents are summarized in Table 2. The crystallite-free zones on membranes M1 and M4 yielded Ag concentrations close to the overall EDX values. However, the protruding crystallites were much stronger Ag-depleted with average deficits of nearly 7 at.% on M1 and more than 11 at.% on M4 with respect to crystallite-free zones. In comparison with XRD values the discrepancy amounted even to 10 at.% for M1 and 15 at.% for M4. Considering that sampling depth and width of the electron beam were both on the order of 1 µm, Ag deprivation of the surficial particles could have been even larger because of contributions from beneath and around the crystallites to the EDX signal. Obviously, Ag deficiency of those crystallites contributed significantly to the difference between EDX and XRD analyses after operation under H_2 at higher temperatures.

Table 2. Silver concentrations of segregated crystallites and crystallite-free PdAg membrane regions from EDX spot analyses marked in Fig. 5.

Membrane M1		Membrane M1		Membrane M4	
spot no.	Ag at.%	spot no.	Ag at.%	spot no.	Ag at.%
1	17.7	3	24.4	11	18.1
2	16.5	4	21.5	12	10.4
5	17.3	9	25.7	13	9.6
6	18.5	10	26.6	14	9.1
7	17.7			15	10.9
8	18.3			16	3.6

In contrast, XPS has a probing depth of a few nm only and thus provides information about the near-surface region. Ag contents of the binary alloys derived from Pd3d and Ag3d XPS spectra of the membrane fragments are included in Table 1. Accordingly, Ag was overall enriched in the near-surface region of the membranes both after annealing in H_2 at 823 K and 873 K. Fig. 6 shows Ag depth profiles of the near-surface regions of membranes M1 and M2 obtained from XPS analyses with intermittent Ar ion sputtering. In both cases Ag enrichment was limited to a few nm below the surface. Overall, silver concentrations exceeded bulk XRD and EDX values by 10-20% in the near-surface region suggesting that neither the 50 K higher temperature nor surficial crystallite segregation had significant impact on the near-surface composition of the PdAg layers.

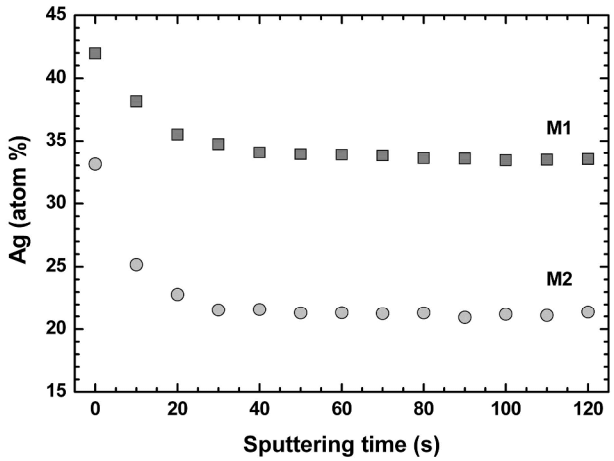

Fig. 6 Surface Ag concentration depth profiles of membranes M1 and M2 from Pd3d and Ag3d XPS analyses with intermittent Ar^+ ion sputtering.

4. Discussion

The steady H_2 flux of Pd membrane M5 at 873 K shows that the declining permeation rate of the alloy membranes was rooted in the instability of the PdAg layer under the same conditions. Surface enrichment with Ag has been previously invoked as explanation when the H_2 permeation rate of a PdAg membrane dropped by 50% after raising the temperature from 823 K to 923 K.[16] Silver accumulation at the surface is minimal according to our results, being limited to a few nm at the outermost surface (Fig. 6). Moreover, it was enriched to similar degrees in the near-surface region of all membranes after operation under H_2 both at 823 K and 873 K (Table 1), respectively. This is consistent with studies by Cornaglia and co-workers who further demonstrated that near-surface Ag concentrations gradually declined with increasing temperature above 748 K in accordance with thermodynamic principles.[24,25] Such thin layers could be much faster accumulated and dispersed above 823 K than implied by the slow H_2 flux decline and recovery of membrane M2 during annealing under H_2 and N_2 (Figs. 1 and 2). For example, H_2 permeation rates became stable within 24 h while alloying Pd membranes with 20-30 nm thick Au layers under H_2 at 773 K.[28] Thus, the dwindling of H_2 fluxes above 823 K cannot be ascribed to excessive Ag accumulation near the membrane surface.

The time scale of H_2 flux decline and its reversal is much more compatible with growth and dissolution of surficial crystallites in the μm range than formation and dispersion of layers in the low nm regime. Therefore we surmise that the extensive textural changes and deeper reaching stoichiometric variations at the PdAg layer surface were primarily responsible for the steady H_2 flux decline above 823 K and concomitant rise of activation energy during annealing in H_2. It is obvious that H_2 fluxes will be reduced at crystallite sites because membrane thickness is effectively increased there. Furthermore, the stoichiometry of the membranes tested at 873 K and 923 K was close to the optimum value (23% Ag) for hydrogen permeability.[4] Thus, the permeability of the Ag-deficient zones at the membrane surface was significantly lower and increasingly limited the overall H_2 permeation rate. The growth of this layer explains also the increasing activation energy for H_2 separation during annealing in H_2 because E_{act} is smallest for $Pd_{77}Ag_{23}$ alloys.[4] These effects impact H_2 permeation the stronger the more surface is covered by crystallites and the closer the stoichiometry at the membrane surface approaches pure Pd. Since crystal growth and Ag depletion are essentially surface effects they also should reduce permeation rates the stronger the thinner the initial PdAg layer is. Yet, the driving force for crystallite segregation and Ag depletion is not immediately evident

We are not aware of previous reports on segregation of particles with differing alloy stoichiometry from PdAg surfaces under H_2 in the literature. This phenomenon is rather peculiar because Pd and Ag form homogeneous solid solutions over the entire binary composition range and the same is generally accepted for the ternary Ag-H-Pd system at temperatures above 573 K.[29] A miscibility gap exists in the ternary phase diagram below that threshold but it narrows with increasing Ag content and is suppressed below room temperature if Ag exceeds 25% in the underlying binary alloy.[5,29] In addition, there are no reports concerning a concomitant change of PdAg stoichiometry upon segregation of these low-temperature PdAg hydride phases. Thus, thermodynamic instability of involved PdAg hydride phases does not appear to be the driving force for the here observed segregation phenomena at high temperatures and moderate H_2 pressures.

Segregation could be triggered by contamination of the PdAg layer with other metals. Okazaki et al. observed declining H_2 fluxes upon operating Pd and PdAg membranes supported on Al_2O_3 substrates under H_2 at 873 K and subsequently detected Al via XPS in the metal layers.[14,30] From this they inferred reduction of the ceramic support and attributed the flux decline to formation of less permeable PdAl alloys.[14,30] The PdAl like the PdZr phase diagram consists of many discrete phases[31,32] and segregation of such crystallites from an otherwise homogeneous PdAg alloy would be plausible. However, we detected neither Al nor Zr in our EDX analyses of the crystallites. In addition, H_2 permeation rates remained steady when Okazaki and co-workers tested Pd membranes supported on yttrium-stabilized zirconia (YSZ) in H_2 up to 923 K.[30] Diffusion barriers made of YSZ proved to be also stable during testing of Pd membranes on stainless steel supports in H_2 at 873 K while Ti was found in the noble metal layer after testing TiO_2 barriers under the same conditions.[33] Therefore, the ZrO_2 layer beneath the Pd and PdAg membranes should have prevented support reduction in our study, too, and the H_2 flux of Pd membrane M5 was indeed stable during annealing in H_2 at 873 K. Hence, metal contamination of the hydrogen-selective PdAg layers due to instability of the metal/ceramic composite structure under H_2 is dismissed as cause of particle segregation and deteriorating H_2 permeability in the present case as well.

On the other hand, numerous surface science studies have shown that Ag begins to sublimate from PdAg surfaces at temperatures around 873 K.[17,34,35] This is intriguing because nucleation from metal vapours presents a straightforward route to the here observed surficial crystallites. There is no doubt that Ag and Pd vapours would be rapidly oversaturated around 873 K favouring resublimation of vaporised metal atoms on the membrane itself. Preferential growth of crystallites on the surface could be triggered by the higher reactivity of freshly nucleated, hydrogen-free crystallite surfaces towards metal atoms.

Silver depletion of the segregated crystallites can be also understood if Ag sublimates faster from PdAg hydrides than Pd as it is the case for the hydrogen-free alloys. Silver can be replenished at the surface via diffusion from the underlying bulk. Thus alloy composition in the surface region depends on the balance between metal sublimation rates and bulk metal diffusion rates. Apparently the former become noticeably larger than the latter around 873 K in PdAg hydrides. Note that the large surface-to-volume ratio of μm-sized particles facilitates Ag sublimation while the relatively small crystallite volume constitutes a limited Ag reservoir. Hence, Ag could be much faster depleted in particles in comparison to the PdAg layer underneath once they have formed. Thus, our experimental key observations can be readily rationalized on basis of a sublimation/resublimation sequence.

Yet, particle segregation and Ag depletion towards the surface were reversed as well as the decline of E_{act} and H_2 permeation rate when operating the membrane under N_2. This can be understood if the activity of Ag and Pd was noticeably enhanced in PdAg hydrides compared with binary PdAg alloys, i.e. metal

vapour pressures should be higher over the hydrides. In addition the balance could be different between e.g. Ag sublimation rate and bulk alloy Ag diffusion rate in metallic and hydrogenated PdAg phases, i.e. metal diffusion rates could remain higher than sublimation rates in hydrogen-free PdAg in the investigated temperature range. Under these conditions Ag will be replenished in the deficient zone near the membrane surface through diffusion from the interior PdAg layer when switching from H_2 to N_2 atmosphere as observed for M1 fragments. Furthermore, the composition of M1 fragments annealed in N_2 remained comparable to the one determined by XRD despite of the Ag loss under H_2. This indicates that the Ag-deficient zone near the membrane surface remained small relative to overall PdAg layer thickness after 240 h operation in H_2 at 873 K so that overall alloy stoichiometry had not changed markedly after equilibration of the Ag distribution under N_2 atmosphere.

Unfortunately, metal activities have only been studied for PdAg alloys but not for PdAg hydride phases to the best of our knowledge. The Pd activity deviates positively from ideal behaviour in Pd-rich binary PdAg alloys at 923-1023 K while the Ag activity deviates negatively at 1000 K.[36-38] Thus Pd sublimation is facilitated and Ag sublimation hampered from the here investigated alloys relative to the pure metals. This leads to some convergence of the metal vapour pressures over the alloys since Ag vapour pressure is noticeably higher than that of Pd over the elements at 873-923 K. On the other hand, Pd and Ag are commonly alloyed under hydrogen atmosphere during preparation of supported membranes[9-11] in order to accelerate this process at low temperatures. Shu et al. showed that the presence of hydrogen favours the Pd-Ag interdiffusion and leads to substantial reduction of the associated activation energy.[9] This observation indicates that intermetallic bonding is weakened in PdAg hydrides and suggests that metal activities in these phases indeed are increased with respect to the hydrogen-free alloys. Therefore, the segregation effects are likely reverted in the absence of H_2 because metal sublimation rates remain too low in metallic PdAg to overtake bulk metal diffusion rates and obstruct homogeneous alloying in the investigated temperature range effectively.

Of course, the metal sublimation/resublimation sequence can play out at the metal/ceramic interface, too, where it may impact membrane behaviour even stronger. The ceramic substrate provides ample sites for nucleation of metal vapours so that Ag could be lost faster from the interfacial PdAg surface than the opposite one. Moreover, the extent to which sublimation occurs, and these surface effects are noticed, likely will depend on alloy layer thickness and stoichiometry as well as operation conditions like H_2 partial pressures and H_2 pressure gradient across the membrane. Indeed, H_2 permeation through thick, self-supported PdAg foils may be hardly affected over long time scales because of permeation rates being entirely governed by bulk hydrogen diffusion. Nevertheless, our findings cast doubt on the stability and practical applicability of thin-layered, supported PdAg membranes for H_2 separation above 823 K.

5. Conclusions

The H_2 flux of PdAg/ceramic composite membranes with less than 10 µm thick alloy layers decreased continuously with time during operation under H_2 above 823 K. This was accompanied by a steady increase of the activation energy for H_2 permeation and the growth of Ag-depleted crystallites on the membrane surface. However, hydrogen permeation rates could be largely restored and the changes of surface morphology reversed through annealing under N_2 above 823 K. These observations can be understood if the metals sublimate from hydrogenated PdAg layers at higher temperatures which is known to occur for hydrogen-free PdAg crystals. Resublimation and nucleation of metal vapours could lead to the observed growth of crystallites on the membrane surface. The decline of H_2 permeation rate and increase of associated activation energy can be attributed to the ensuing textural and stoichiometric inhomogeneity. This segregation mechanism implies an enhancement of the yet unknown activity of Ag and Pd in PdAg hydride phases over that in the underlying binary alloys. Hence, studies on the activity of metals in such hydrides are highly desirable to further elucidate the behaviour of metal membranes and improve their stability under high-temperature H_2 separation conditions.

Acknowledgement

Financial support by the Chinese Academy of Sciences through the External Cooperation Program (Helmholtz-CAS Joint Research Group on Integrated Catalytic Technologies for Efficient Hydrogen Production, grant no. GJHZ1304), the National 863 Project (grant no. 2012AA050104) and the Ministry of Science and Technology of China (grant no. 2005CB221401) is gratefully acknowledged.

Notes and references

[a]*Dalian National Laboratory for Clean Energy, Dalian Institute of Chemical Physics, Chinese Academy of Sciences, Zhongshan Road 457, 116023 Dalian, China, Fax: +86 411 8469 1570; Tel:+86 8437 9229; E-mail: goldbach@dicp.ac.cn (A. Goldbach); xuhy@dicp.ac.cn (H. Xu).*
[b]*CAS Key Laboratory of Low-carbon Conversion Science and Engineering, Shanghai Advanced Research Institute, Chinese Academy of Sciences, Shanghai, 201210,China.*
[c]*State Key Laboratory of Functional Materials for Informatics, Shanghai Institute of Microsystem and Information Technology, Chinese Academy of Sciences, Shanghai 200050, China*

† Electronic Supplementary Information (ESI) available: [details of any supplementary information available should be included here]. See DOI: 10.1039/b000000x/

‡ Authors G. Zeng and H. Jia contributed equally.

1 J. A. Ritter and A. Ebner, *Sep. Sci. Technol.,* 2007, **42**, 1123.
2 F. Galluci, E. Fernandez, P. Corengia and M. van Sint Annaland, *Chem. Eng. Sci.,* 2013, **92**, 40.
3 G. L. Holleck, *J. Phys. Chem.,* 1970, **74**, 503.
4 G. Zeng, A. Goldbach, L. Shi and H. Xu, *J. Phys. Chem. C*, 2012, **116**, 18101.
5 Y. Sakamoto, K. Yuwasa and K. Hirayama, *J. Less-Common Met.,* 1982, **88**, 115.
6 S. N. Paglieri and J. D. Way, *Sep. Purif. Rev.*, 2002, **31**, 1.
7 S. Yun and S. T. Oyama, *J. Membr. Sci.,*2011, **375**, 28.
8 H. W. Abu El Hawa, S. N. Paglieri, C. C. Morris, A. Harale and J. D. Way, *J. Membr. Sci.*, 2014, **466**, 151.
9 J. Shu, A. Adnot, B. P. A. Grandjean and S. Kaliaguine, *Thin Solid Films,* 1997, **286**, 72.
10 M. E. Ayturk, E. A. Payzant, S. A. Speakman and Y. H. Ma, *J. Membr. Sci.,* 2008, **316**, 97.
11 G. Zeng, A. Goldbach, L. Shi and H. Xu, *Int. J. Hydrogen Energy*, 2012, **37**, 6012.

12 O. Iyoha, R. Enick, R. Killmeyer, B. Howard, B. Morreale and M. Ciocco, *J. Membr. Sci.,* 2007, **298**, 14.

13 R. Dittmar, A. Behrens, N. Schlödel, M. Rüttinger, T. Franco, G. Straczewski and R. Dittmeyer, *Int. J. Hydrogen Energy,* 2013, **38**, 8759.

14 J. Okazaki, T. Ikeda, D. A. Pacheco Tanaka, K. Sato, T. Suzuki and F. Mizukami, *J. Membr. Sci.,* 2011, **366**, 212.

15 D. Xie, J. Yu, F. Wang, N. Zhang, W. Wang, H. Yu, F. Pen and A. Park, *Int. J. Hydrogen Energy,* 2011, **36**, 1014.

16 Y. S. Cheng, M. A. Peña, J. L. Fierro, D. C. W. Hui and K. L. Yeung, *J. Membr. Sci*., 2002, **204**, 329.

17 P. T. Wouda, M. Schmid, B. E.Nieuwenhuys and P. Varga, *Surf. Sci.,* 1998, **417**, 292.

18 J. Shu, B. E. W. Bongondo, B. P. A. Grandjean, A. Adnot and S. Kaliaguine, *Surf. Sci.,* 1993, **291**, 129.

19 M. Lukaszweski, K. Klimek and A. Czerwinski, *J. Electroanal. Chem.,* 2009, **637**, 13.

20 O. M. Lovvik and S. M. Opalka, *Surf. Sci.,* 2008, **602**, 2840.

21 S. Gonzalez, K. M. Neyman, S. Shaikhutadinov, H.-J. Freund and F. Illas, *J. Phys. Chem. C,* 2007, **111**, 6852.

22 A. A. B. Padama, H. Kasai and Y. W. Budhi, *Int. J. Hydrogen Energy,* 2013, **38**, 14715.

23 T. A. Peters, W. M. Tucho, A. Ramachandran, M. Stange, J. C. Walmsley, R. Holmestad, A. Borg and R. Bredesen, *J. Membr. Sci.,* 2008, **326**, 572.

24 M. L. Bosko, J. B. Miller, E. A. Lombardo, A. J. Gellman and L. M. Cornaglia, *J. Membr. Sci.,* 2011, **369**, 267.

25 A. M. Tarditi, M. L. Bosko and L. M. Cornaglia, *Int. J. Hydrogen Energy,* 2012, **37**, 6020.

26 G. Zeng, A. Goldbach and H. Xu, *J.Membr. Sci.,* 2009, **326**, 681.

27 H. Li, A. Goldbach, W. Li and H. Xu, *J. Membr. Sci.,* 2007, **299**, 130.

28 L. Shi, A. Goldbach and H. Xu, *Int. J. Hydrogen Energy,* 2011, **36**, 2281.

29 P. Perrot, N. Moelans and N. Lebrun, Silver–Hydrogen–Palladium, *in*: Noble Metal Ternary Systems: Phase Diagrams, Crystallographic and Thermodynamic Data. Effenberg, G., Ilyenko, S. (ed.), SpringerMaterials - The Landolt-Börnstein Database (http://www.springermaterials.com). DOI: 10.1007/10916070_17.

30 J. Okazaki, T. Ikeda, D. A. Pacheco Tanaka, M. A. Llosa Tanco, Y. Wakui, K. Sato, F. Mizukami and T. M. Suzuki, *Phys. Chem. Chem. Phys.,* 2009, **11**, 8632.

31 H. Okamoto, *J. Phase Equilib. Diff.,* 2008, **29**, 199.

32 H. Okamoto, *J. Phase Equilib.,* 2002, **23**, 290.

33 Y. Huang and R. Dittmeyer, *J.Membr. Sci.,* 2006, **282**, 296.

34 P. Pervan and M. Milun, *Surf. Sci.,*1992, **264**, 135.

35 T. Marten, O. Hellman, A. V. Ruban, W. Olovsson, C. Kramer, J. P. Godowski, L. Bech, Z. Li, J. Onsgaard and I. Abrikosov, *Phys. Rev. B,* 2008, **77**, 1254061.

36 G. Ghosh, C. Kantner and G. B. Olson, *J. Phase Equilib.*, 1998, **20**, 295.

37 N. G. Schmahl and W. Schneider, *Z. Phys. Chem.*, 1968, **57**, 218.

38 P. K. Raychaudhuri, PhD thesis, Northwestern University, 1971.